Magnetic Attitude Control of Gossamer Spacecraft using a 3D-printed, Electrically Conducting Support Structure

Bonar Robb,[1] Malcolm McRobb,[2] and Colin McInnes[3]
University of Glasgow, Glasgow, Scotland G12 8QQ, United Kingdom

An attitude control strategy for gossamer spacecraft is proposed, where control torques are generated by an electrically conducting support structure interacting with the Earth's magnetic field. A mathematical model of the structure is developed, where the overall torque is found by summation of the Lorentz forces acting upon each current-carrying structural element. Different geometric configurations are shown to allow effective magnetic dipole moments in three orthogonal directions. With this model, the results of dynamic simulation are presented in order to assess the ability of the conducting structure to detumble itself in-orbit, using the classical *Bdot* control law. The possibility of using this attitude control system to manoeuvre orbital reflectors is then investigated. The required angular accelerations for a large solar reflector in polar orbit to continuously illuminate a fixed point on the Earth's surface are derived within a simplified model, and compared with those achievable by the conducting structure. Simulation is then used to assess whether the conducting structure is capable of achieving partial attitude control of an orbital reflector, for example to illuminate terrestrial solar power farms at dawn and dusk when their output is low.

Nomenclature

T	=	Torque, Nm
$\boldsymbol{B}$	=	Magnetic field, T
I	=	Current, A
d	=	Spacecraft side-length, m
L	=	Path segment length, m
σ	=	Areal mass density, g m^{-2}
I	=	Mass moment of inertia, kg m^2
$\boldsymbol{\omega}$	=	Body rates, rad s^{-1}
$\boldsymbol{r}$	=	Satellite position vector
$\boldsymbol{R}$	=	Target ground-point position vector
θ	=	True anomaly, rad
ψ	=	Reflector pitch angle, rad

I. Introduction

Gossamer spacecraft are lightweight structures which support thin, reflective membranes. This paper proposes a novel magnetic attitude control system for gossamer spacecraft which uses an electrically conducting support structure. The concept is motivated by a recent uptake in interest in the prospect of in-orbit fabrication. Strategies have been proposed which combine 3D-printing and robotic manipulators for manufacturing large space structures [1, 2]. This technology would allow the development of gossamer spacecraft at a much larger scale, and lower cost, than is currently feasible with terrestrial manufacturing prior to launch. One possible application of gossamer spacecraft is orbital reflectors [3]. This is a long-standing concept for energy from space which proposes the use of large, planar reflectors to direct sunlight from orbit to terrestrial solar power farms. These orbital reflectors would consist of a lightweight support structure overlaid with a thin reflective film. The support structure could be 3D-printed in-orbit before unrolling

[1]Graduate Student, James Watt School of Engineering, James Watt (South) Building; b.robb.1@research.gla.ac.uk
[2]Research Associate, James Watt School of Engineering, James Watt (South) Building, *currently with AAC Clyde Space*
[3]Professor, James Watt School of Engineering, James Watt (South) Building

and affixing the thin film, or the structure could be printed directly onto the membrane, resulting in a relatively simple fabrication process. Reference [4] discusses some current research on in-orbit fabrication, and the potential for additive manufacturing technologies to be adapted to fabricate large, lightweight structures in space. To operate as orbital reflectors these structures would require appropriate attitude control. The purpose of this paper is to propose an attitude control strategy that could be integrated within the spacecraft structure during in-orbit fabrication.

The most common type of gossamer spacecraft which appears in the technical literature is the solar sail, for which a number of attitude control strategies have been proposed. These include reaction wheels, gimballed counterweight systems and the use of solar radiation pressure via controllable tip vanes or sail elements [5–8]. However, this paper focuses on the use of magnetic control, where Lorentz forces are generated by current carrying elements embedded within the gossamer spacecraft support structure. This type of control could be suitable for application to orbital reflectors, as these would operate in low Earth orbit (LEO) and take advantage of the Earth's magnetic field to provide attitude control.

The concept of orbiting solar reflectors has been discussed since the 1970s, when multiple NASA studies were performed on the physical and economical feasibility of the concept [3, 9]. These reflectors could be used to extend the operating hours of terrestrial solar power farms and so could be of economic benefit, but the economics are highly dependent upon launch costs and reflector design [10]. Development of the concept has included discussion of reflector constellations, and which families of orbits could best deliver power to target solar power farms. Reference [11] proposes a "flower" constellation of reflectors in elliptical orbits which could provide additional solar power to equatorial regions, and develops steering laws for such a constellation. Another design is proposed in Ref. [12], which consists of 18 reflectors in Sun-synchronous polar orbit, with economic assessment that such a system could pay for itself within 0.7 years of the beginning of operations. Reference [13] proposes a design for the reflector itself, consisting of a triangular deployable membrane mirror, controlled by a central bus equipped with control moment gyros for attitude control.

This paper is concerned with magnetic attitude control, as this could serve as a simple, low-cost attitude control system for large reflectors. Reference [14] investigated the use of distributed arrays of magnetorquer rods for the control of large planar structures, showing that magnetic control could provide useful torques for a large space structure, and that there could be significant advantages to distributing actuator torques across a flexible structure. This paper proposes a different method of achieving magnetic control, through the use of a current-carrying support structure, which would also benefit from the advantages of distributed actuator torques.

In Sec. II, the mathematical model of the current-carrying structure is presented, demonstrating how particular geometric current-carrying paths within a square "lattice-type" structure result in control torques acting upon the spacecraft. With physical parameters representative of a large gossamer spacecraft, dynamic simulation is then undertaken using the model to demonstrate that the conducting structure could be used to detumble a 100×100 m structure. Section III then refers back to orbital reflectors, as the application which has prompted the development of this concept. A simplified model is developed to illustrate the operational concept of using these reflectors to enhance terrestrial solar power, and the general attitude control requirements are investigated. A dipole model of the Earth's magnetic field is then used to assess how attitude control of a reflector in a polar orbit could be achieved by the conducting structure concept.

II. Torques Generated by a Square Lattice-Structure with Conducting Paths

The proposed concept consists of a square lattice type structure, with conducting paths embedded within the structural elements. The structure could be 3D-printed in-orbit, and so the conducting paths could be fabricated either by 3D-printing a conducting material directly, or by affixing conducting material to the structure with robotic manipulators after printing. Once printed, a reflective film could be overlaid and attached to the support structure, again with the aid of robotic manipulators, or the structure could even be printed directly onto the film. The spacecraft would also require electrical power to generate a current in the paths, and a central bus for active control and other subsystems. A mathematical model of the conducting structure is now developed, from which the torques generated by the current carrying elements in the presence of an external magnetic field are calculated.

A. Calculation of Torques

Figure 1 shows an illustration of the proposed spacecraft, where a conducting path is shown in red, and winds back and forth across the structure. The spacecraft bus is represented by the blue sphere at the centre-of-mass, and the reflective film is not shown for clarity. The coil path is taken to consist of 3/4 of a turn in the xz-plane, followed by a step in the y-direction which repeats back and forth across the structure, as shown in the expanded view of Fig. 1. The

following analysis refers to a list of nodes which sequentially describe this path. The force on an individual path segment between points with indices i and $i+1$, in the presence of an external magnetic field $\boldsymbol{B}$, is given by the Lorentz force law:

$$\boldsymbol{f}_i = I\,\boldsymbol{L}_i \times \boldsymbol{B} \tag{1}$$

where $\boldsymbol{L}_i$ is a vector with magnitude equal to the segment length and aligned from i to $i+1$, and I is the current. The expanded view in Fig. 1 shows the first points in the path sequence, from which it is evident that this vector is given by the difference in position of points i and $i+1$. Position vectors are taken from the centre-of-mass of the spacecraft, such that:

$$\boldsymbol{L}_i = \boldsymbol{r}_{i+1} - \boldsymbol{r}_i \tag{2}$$

To calculate the torque contributed by this line segment, it is assumed that the entirety of the force acts upon the midpoint of the line segment rather than being distributed evenly across the path element. This assumption is made since the segment length is small compared to the overall spacecraft side length. In this case, the torque contributed by path segment i is given by:

$$\boldsymbol{\tau}_i = \frac{1}{2}(\boldsymbol{r}_i + \boldsymbol{r}_{i+1}) \times (I\,\boldsymbol{L}_i \times \boldsymbol{B}) \tag{3}$$

The total torque generated by the conducting path is then found by summation over the n individual segments:

$$\boldsymbol{T} = \sum_{i=1}^{n-1} \frac{1}{2} I\,(\boldsymbol{r}_i + \boldsymbol{r}_{i+1}) \times [(\boldsymbol{r}_{i+1} - \boldsymbol{r}_i) \times \boldsymbol{B}] \tag{4}$$

where the sequence $\{\boldsymbol{L}_1, ..., \boldsymbol{L}_n\}$ is defined by the geometry of the structure and the connections between the conducting pathways.

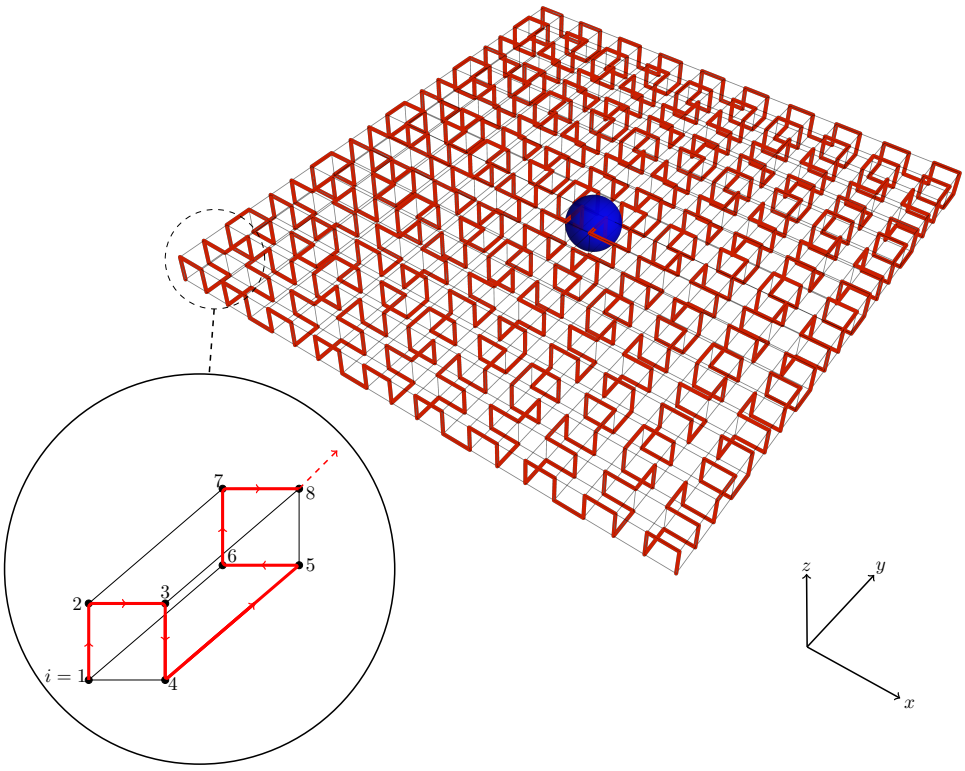

Fig. 1 A cubic lattice support structure with an embedded conducting path shown in red. Interaction between the structure's current-carrying elements and the Earth's magnetic field generates torques which may then be used for attitude control. The blue sphere represents the spacecraft bus. The expanded image illustrates the first points in the path sequence on a segment of the structure.

For a square structure such as that shown in Fig. 1, with physical data given in Table 1, the maximum achievable torque would be 1.12 Nm. The magnetic field strength in Table 1 is taken to be 30 μT as this is a typical value for LEO [15], and the areal mass density, σ, assumes an ultra-lightweight structure, composed of a 3D-printed polymer or composite material, overlaid with a thin film. This areal density may in fact be a conservative estimate, as solar sails with areal densities on the order of 10 g m^{-2} have been proposed [10]. However, a higher value was used for this paper as it is expected that the mass of conductor required to carry a current of 10 A would increase the areal mass density significantly. Further work would be required to assess the feasibility of fabricating a functional spacecraft of this density and scale in orbit, however these values are used to provide an order of magnitude estimate of the potential torques achievable.

Side length	d	100m
Path segment length	L	1m
Field Strength (LEO)	B	30 μT
Current	I	10 A
Areal Mass Density	σ	100 g m^{-2}

Table 1 Example spacecraft configuration.

It is also possible to envision multiple conducting paths within the structure, allowing torques to be generated in more than one axis. Typically, magnetic attitude control systems consist of three orthogonal coils, allowing torques to be generated in any direction in the plane perpendicular to the magnetic field. The equivalent for the conducting structure, would be to have to orthogonal coiled paths within the structure, complemented by large current loops lying in

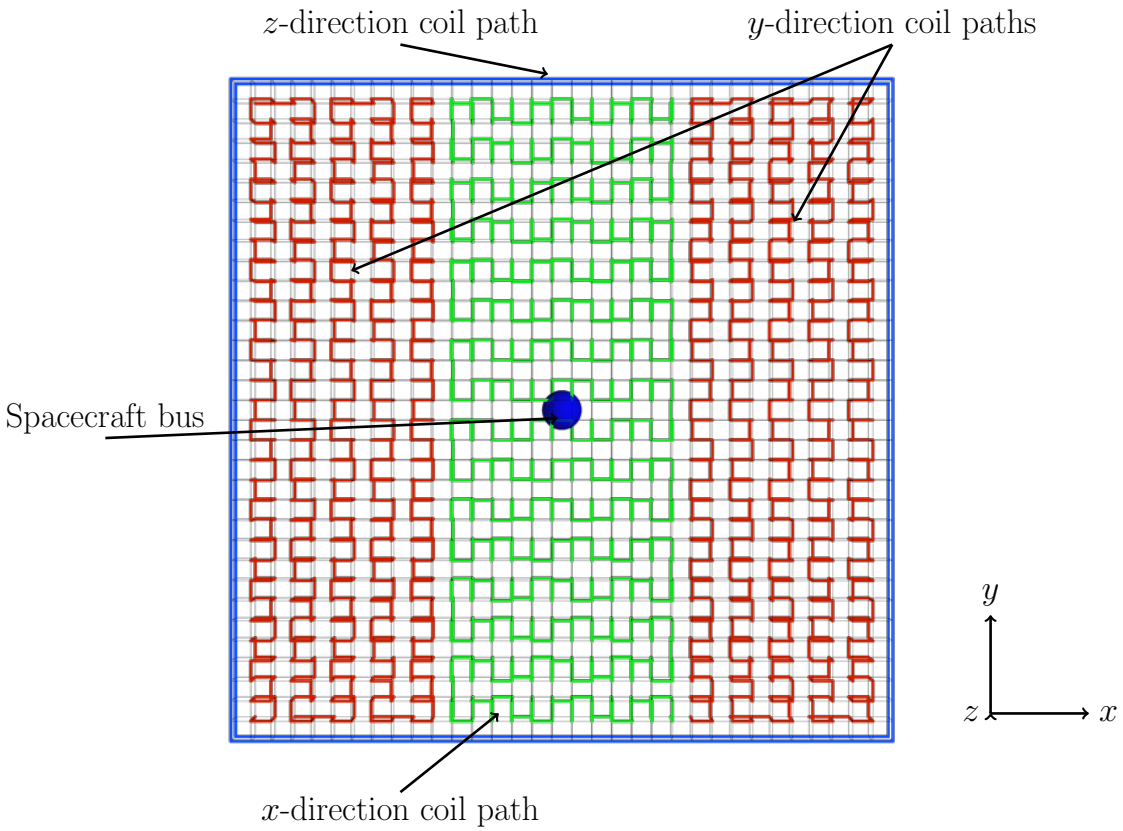

Fig. 2 A conducting structure with 3 different conducting paths. An "effective" magnetic dipole moment is given in the x direction by the green path, the y direction by the red, and z direction by the blue path.

the plane which encircle the structure. Figure 2 illustrates this concept, where the different coloured paths generate torques in orthogonal directions when current is passed through them. While the paths in Fig. 2 are separated into different sections of the structure for illustration, it would be possible to have the different sections overlapping by having multiple insulated paths affixed to the same structural elements.

A further refinement of the concept could entail placing addressable switches at each node of the square lattice. These switches could then be commanded to change the current-path direction as required, depending on the direction of the desired control torque. This would then allow the maximum conducting path length to be used for torque generation in all directions, with a lower mass than having multiple conducting paths as the same conducting elements are used for each coil direction.

B. Detumbling Simulation of a Conducting Structure In-Orbit

The utility of the conducting structure as an attitude control system is now assessed by simulating a square structure in-orbit, with control torques generated by the representative model defined in Table 1. The structure is taken to be a rigid-body, and so the system dynamics are described by the Newton-Euler equations:

$$\mathbf{I}\dot{\boldsymbol{\omega}} + \boldsymbol{\omega} \times (\mathbf{I}\boldsymbol{\omega}) = \boldsymbol{T} \tag{5}$$

where $\boldsymbol{T}$ is the external torque acting upon the spacecraft, $\mathbf{I}$ is the inertia tensor and $\boldsymbol{\omega}$ the angular rates expressed in the principal-axes frame. The dynamics are implemented along with the quaternion kinematic equations:

$$\dot{q} = \frac{1}{2} q[0, \boldsymbol{\omega}] \tag{6}$$

where q is the quaternion describing the current attitude, and $[0, \boldsymbol{\omega}]$ is a quaternion with scalar component 0, and vector part $\boldsymbol{\omega}$, the angular velocity components in the principal axes frame [16]. The equations of motion are implemented in the *MATLAB* programming environment, and solved numerically with the *ode45* integrator. Again, the physical data is taken from Table 1, and the inertia tensor taken to be that of a rigid, flat square plate, given by:

$$\mathbf{I} = \begin{pmatrix} \frac{1}{12}md^2 & 0 & 0 \\ 0 & \frac{1}{12}md^2 & 0 \\ 0 & 0 & \frac{1}{6}md^2 \end{pmatrix} \tag{7}$$

where $m = \sigma d^2$ is the total mass of the structure, d the sidelength and σ the areal mass density. The components of the tensor then have values $I_1 = I_2 = 8.3 \times 10^5$ kg m^2 and $I_3 = 16.7 \times 10^5$ kg m^2. In order to assess the ability of

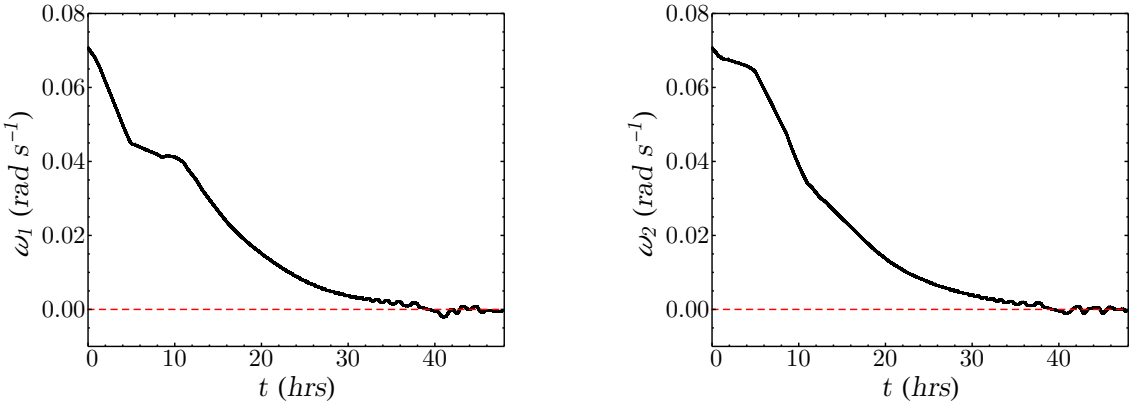

Fig. 3 Body rates of the structure over the simulation time of two days. The structure is detumbled from an initial angular velocity vector of $\omega = (0.707, 0.707, 0)$ rad s^{-1}, nearly to rest.

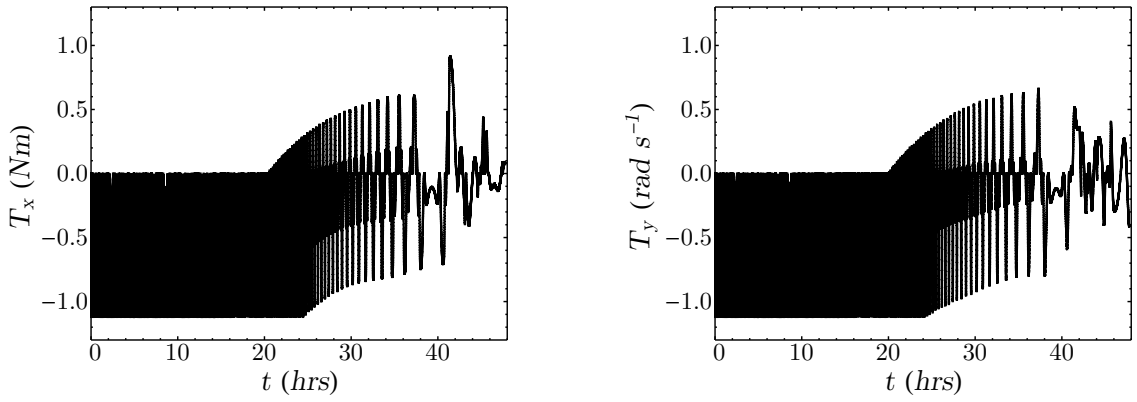

Fig. 4 Torques produced by the conducting structure during simulation. Initially the controller is delivering the maximum torque of 1.12 Nm until the end of the detumbling phase when finer control is required.

the conducting structure to detumble itself, the well-known *Bdot* control law [17] is implemented, which provides an expression for the desired control torque, $\boldsymbol{T}_{Bdot}$, in terms of the body rates, $\boldsymbol{\omega}$, of the spacecraft and the magnetic field, $\boldsymbol{B}$, such that:

$$\boldsymbol{T}_{Bdot} = k\boldsymbol{\omega} \times \boldsymbol{B} \tag{8}$$

for some fixed gain k. This torque is used as the external torque $\boldsymbol{T}$ in Eq. (5), and no other disturbing torques are considered at present. The field direction is taken to be constant throughout the simulation for ease of illustration. The initial angular velocity of the structure is set to $\boldsymbol{\omega} = (0.707, 0.707, 0)$ rad s^{-1}, such that the magnitude of the initial angular velocity is 0.1 rad s^{-1}, a significant spin rate for a 100×100 m structure. The simulation is performed over two days. The geometry of the structure is taken to be two overlaid conducting paths, with orthogonal coil directions, i.e. the path shown in Fig. 1 overlaid with a duplicate path rotated by 90°. The maximum torque generated by each path is 1.12 Nm, as calculated using Eq. (4). A further assumption is that the current in the paths can be varied between zero and a maximum of 10 A, and that the direction of the current can be reversed, allowing the torque magnitude to be varied and the direction to be reversed.

Results of the simulation are shown in Fig. 3, demonstrating that the conducting structure is able to detumble itself in just under two days. The torques are shown in Fig. 4, where it can be seen that initially the controller is delivering the maximum torque of 1.12 Nm when required, until the end of the simulation when the angular rates are reduced sufficiently that finer control is required. It is important to note that the initial angular velocity in the field direction, in this case the z-axis, is zero, as magnetic control is not capable of producing torques in the magnetic field direction and so any angular momentum in this direction would remain after detumbling.

III. Attitude Control of a Reflector in Polar Orbit

The conducting structure concept was motivated by considering an application to orbiting solar reflectors. An investigation is now made of whether the attitude control system could, at least partially, provide the torques required to continuously illuminate a fixed point on the Earth's surface. For this analysis, a simplified model is used to provide an illustration of the operational concept, and to provide a representative example of the angular rates and accelerations required. The purpose of this analysis is to demonstrate that the magnitude of the torque produced by a conducting structure in polar orbit within a dipole magnetic field could be sufficient to control the reflector, and to demonstrate operation by simulating the system over multiple orbits.

A. Attitude Requirements for Simplified Reflector System

Figure 5 shows the geometry of an orbiting solar reflector in a circular, polar orbit. The figure shows the orbital plane, to which we ascribe the coordinate system xyz. This coordinate system is Earth centered and rotates with the orbital plane, such that the y direction always points towards the Sun. The following simplifications are made: 1) the orbit is Sun-synchronous, 2) the tilt of the Earth's axis relative to the ecliptic is ignored, and is taken to be around the z-axis, and 3) the Earth's magnetic field is a dipole field, also centered on the z-axis. The target ground-point which is to be illuminated by the reflector is located at $\boldsymbol{R}$, which changes over time as the Earth rotates. This is assumed to be a large equatorial terrestrial solar power farm. The reflector position is given by vector $\boldsymbol{r}$, and so $\boldsymbol{r}_{rad} = \boldsymbol{r} - \boldsymbol{R}$ is the relative position of the target ground-point and reflector, and the direction in which sunlight is to be reflected. Within this simplified model, the position vectors are given by:

$$\boldsymbol{r} = \begin{pmatrix} r\cos\theta \\ 0 \\ r\sin\theta \end{pmatrix} \tag{9}$$

$$\boldsymbol{R} = \begin{pmatrix} R_e\cos\omega_e t \\ R_e\sin\omega_e t \\ 0 \end{pmatrix} \tag{10}$$

where θ is the true anomaly of the reflector, which changes at a constant rate, as shown in Fig. 5, and R_e, ω_e are the radius and angular velocity of the Earth, respectively. The magnetic field components in the orbital plane are those of a

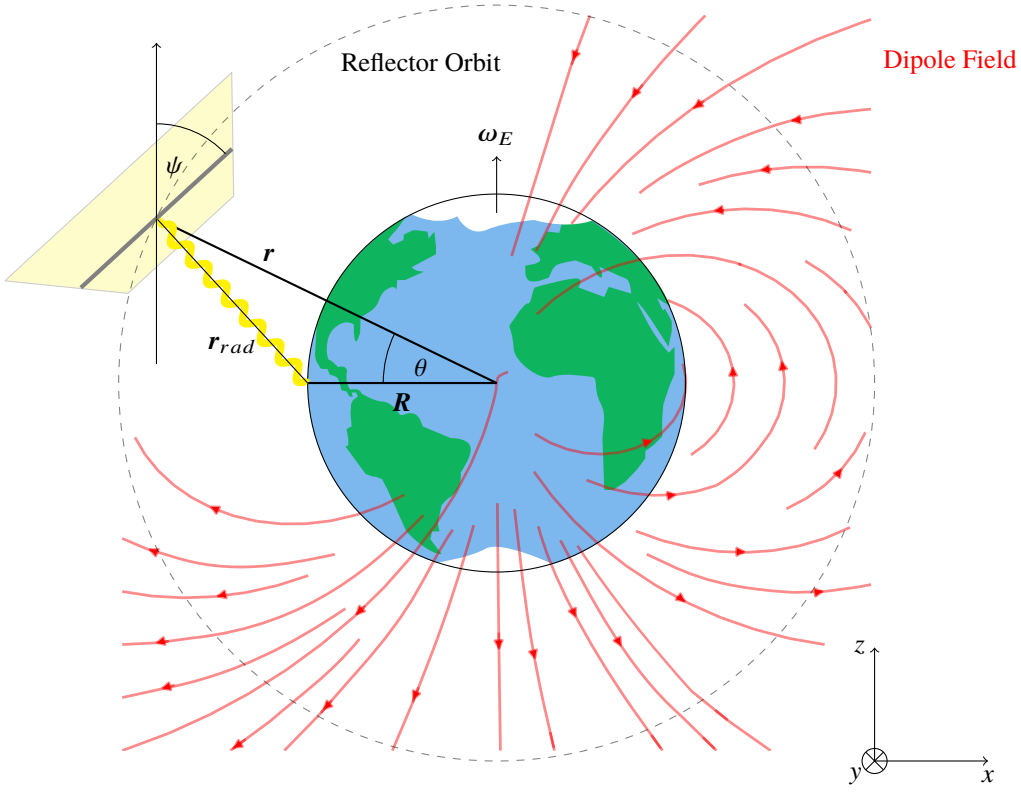

Fig. 5 Geometry of a reflector on a circular, polar orbit, illuminating a point on the Earth's equator. The Earth-Sun vector is in the y direction, so the Sun's radiation is directed into the page. The dipole magnetic field, shown in red, is hidden in the top left of the figure for clarity and is not shown to scale.

dipole field, with polar components given by:

$$B_r = -2B_0 \left(\frac{R_e}{r}\right)^3 \sin\theta$$
$$B_\theta = -B_0 \left(\frac{R_e}{r}\right)^3 \cos\theta \tag{11}$$

where $B_0 = 3.12 \times 10^{-5}$ T is the mean value of the magnetic field at the magnetic equator on the Earth's surface [18]. The angle ψ lies between the z-axis and the line of intersection between the reflector surface and the orbital plane. This line of intersection is shown in grey in Fig. 5. For sunlight incoming along the y-direction to be reflected along $\boldsymbol{r}_{rad}$ to the target ground-point, this line of intersection must be perpendicular to $\boldsymbol{r}_{rad}$, which defines the angle ψ. An expression for ψ is now sought, as this angle needs to be maintained by applying control torques with the conducting structure. The constraints made on the system for this model allow us to consider only the 2D geometry of the xz plane to find this expression. Figure 6 shows the geometry in the orbital plane, where R_x is the projection of the ground-point position onto the plane. An equation for ψ can then be found as:

$$\psi = \frac{\pi}{2} - \varepsilon = \frac{\pi}{2} - \tan^{-1}\left(\frac{r\cos\theta - R_e\cos\omega_e t}{r\sin\theta}\right) \tag{12}$$

As the time dependence of θ is known, it is then possible to find an expression for the required angular velocity of the solar reflector by taking the time derivative of Eq. (12), resulting in:

$$\dot{\psi} = \frac{-rR_e\omega_e \sin(\omega_e t)\sin\theta + r\dot{\theta}(r - R_e\cos(\omega_e t)\cos\theta)}{r^2 + R_e\cos(\omega_e t)(R_e\cos(\omega_e t) - 2r\cos\theta)} \tag{13}$$

An exact expression for the angular acceleration can also be found by taking the time derivative again, omitted here for conciseness.

Equation (12) provides a steering law for the pitch around the Sun-reflector axis which must be maintained. Additionally, the reflector must be angled correctly towards the Sun to provide the required angle of reflection towards the target. In Fig. 5, the reflector, represented by the yellow plane, would be angled at 45° to the page since the target is positioned in the xz plane. This ensures that $\boldsymbol{r}_{rad}$ would be perpendicular to the sun-line direction, providing an

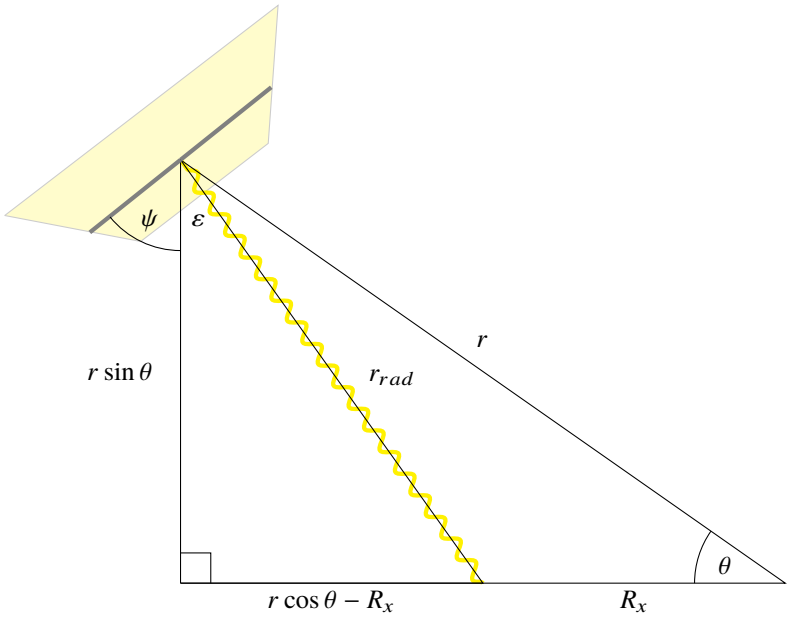

Fig. 6 Geometry of the reflector-target vector $\boldsymbol{r}_{rad}$, illustrating how the angle ψ can be determined

angle of reflection of 45°. As the ground point rotates with the Earth and moves out of the orbital plane, the reflector would need to roll around the reflector axis shown in grey in Figs. 5 and 6 to give the correct angle of reflection. This component of the reflector attitude dynamics is ignored in this analysis because this angle changes at a much slower rate than the angle ψ, since changes in this angle depend on the target ground-point velocity, while changes in ψ depend mainly upon the reflector orbital velocity which is much faster. Another reason this component of the attitude dynamics is ignored is because it would require control torques with a component in the z-direction. A torque in this direction could not always be achieved due to the fact that torques can only be produced in the plane normal to the field direction, which is an inherent constraint of magnetic attitude control. If the conducting support structure is found capable of maintaining the pitch angle ψ, it could then be supplemented by reaction wheels or another attitude control system to achieve the required angle of reflection.

B. Attitude Control of an Orbiting Solar Reflector

A simulation is now performed of a conducting gossamer structure in orbit, with torques generated by the conducting paths which attempt to maintain the structure attitude such that the angle ψ, given by Eq. (12), is continually maintained. The physical data given in Table. 1 is again assumed. Rather than the *Bdot* controller used previously to detumble the structure, a quaternion error feedback controller is now used to generate control torques, with the desired orientation specified by Eq. (12). The control law is given by:

$$\boldsymbol{T}_{ref} = -P_q \boldsymbol{q}_{\text{err}} - P_\omega \boldsymbol{\omega} \tag{14}$$

where P_q and P_ω are the controller gains, $\boldsymbol{\omega}$ the angular rates, and

$$\boldsymbol{q}_{err} = \boldsymbol{q}_{ref} \boldsymbol{q}_t^* \tag{15}$$

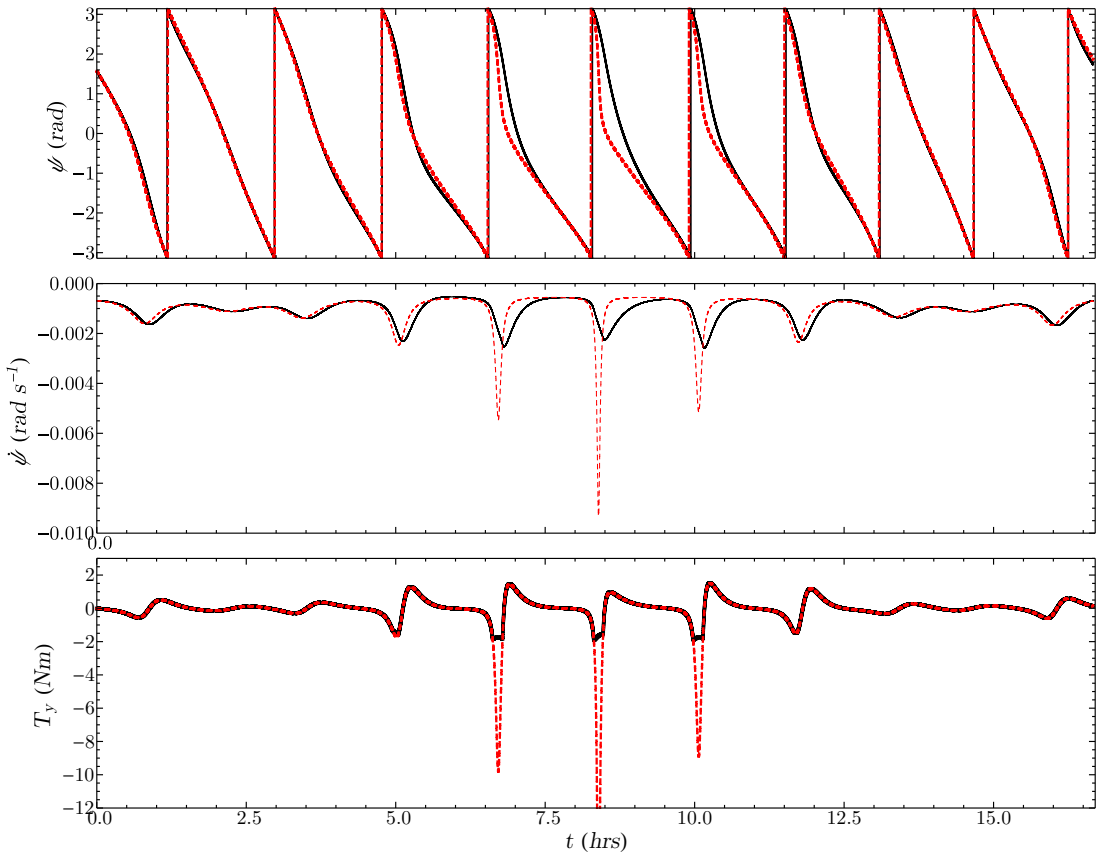

Fig. 7 Results of simulation for a 100×100 m orbiting solar reflector, showing the conducting structure is only capable of maintaining the required pitch angle ψ for part of the simulation. Actual values are shown in black with reference values shown in red.

is the error quaternion, given by quaternion multiplication between the current attitude, $\boldsymbol{q}_t$, and the desired, $\boldsymbol{q}_{ref}$. This generates a reference torque, and the nearest achievable torque which can be generated by the conducting structure is used to propagate the Newton-Euler equations. The nearest achievable torque is found by assuming that again the structure consists of two overlaid paths, described in Sec.II, with the addition of a third path consisting of coils lying in the plane of the structure, shown in blue in Fig. 2, also capable of producing 1.12 Nm. With this geometric configuration, analogous to having three perpendicular magnetorquers, a torque can be generated in any direction in the plane normal to the magnetic field direction. To find the actuator torque, the reference torque is projected onto the plane normal to the magnetic field and is then taken to be the torque generated by the array, up to the maximum achievable torque calculated by Eq. (4). This torque is then used to propagate the Newton-Euler equations. A key difference to the previous detumbling simulation is that the magnetic field direction is no longer constant, instead it's components are given by Eq. (11). Due to the constrained geometry of the system, these torques will always lie on the y-axis, and so deliver an angular acceleration around the Sun-reflector direction. The orbital altitude is taken to be 800 km, resulting in an orbital period of 100.7 minutes. The simulation is performed for 10 orbital periods, and so 10 passes of the ground-point are made, and the initial position of the ground-point is chosen such that halfway through the simulation it is located directly underneath the reflector. The attitude control system attempts to point towards the target ground-point even when it is not visible from the reflector, as this ensures the reflector will have the correct orientation when the ground-point next becomes visible. Results of the simulation are shown in Fig. 7. The attitude control system is able to maintain the required pitch angle, ψ, until around $t = 5.5$ hrs. This is because at this point, the required torque exceeds the torque achievable by the structure, and so the angular acceleration of the reflector lags behind that required by Eq. (12). The results show that larger torques are required around the halfway point of the simulation. This is because, at this time the ground-point has rotated with the Earth into the orbital plane, and so is directly underneath the reflector. Since the distance between the reflector and target is then much lower, the reflector must rotate faster to maintain illumination.

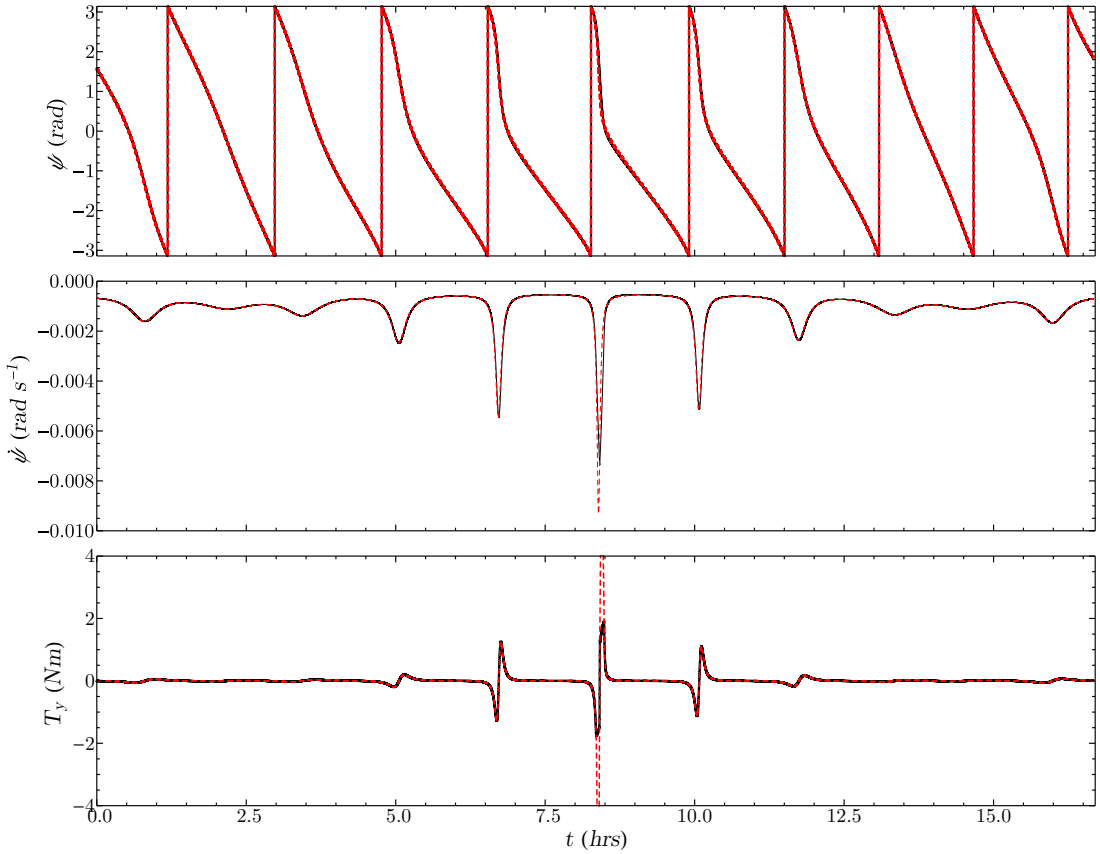

Fig. 8 Results of simulation for a 100×100 m orbiting solar reflector with areal density of 10 g m^{-2}, showing that a maximum torque of 2 Nm is now sufficient to maintain the required pitch angle ψ.Actual values are shown in black with reference values shown in red.

However, other than the three passes nearest this point, the system is capable of producing the required torques.

As discussed previously, the areal mass density value of 100 g m^{-2} used in this work is an order of magnitude higher than that which may be assumed for solar sails, and was a conservative value chosen by assuming that the conducting mass required to fabricate this structure would increase the density substantially. If it were possible to fabricate a structure with an areal density of 10 g m^{-2}, this would decrease the moments of inertia by a factor of 10. Such a structure was simulated and results are shown in Fig. 8. Due to the lower mass, the maximum torque achievable by the conducting structure is now sufficient to provide the required attitude control, as the values of ψ and $\dot{\psi}$ are now seen to match the reference values for the duration of the simulation. When the reflector passes directly over the ground-point, at $t = 8.3$ hrs, the torque can still not match the reference reference torque, however this is seen to have minimal effect on the error in ψ, as the reference torque is not achieved for only a small period of time. While it remains to be seen whether a conducting structure capable of conducting 10 A of current could be realised, even the results for a structure with an areal density of 100 g m^{-2} demonstrate that at the required pitch angle could be achieved by this system for the majority of the reflector's operation. The reflector could then be supplemented by another attitude control system for the time period when the reflector passes directly over the target, and for fine-pointing.

IV. Conclusion

From the analysis presented in this paper, we conclude that a conducting support structure, delivering magnetic torques by interaction with the Earth's magnetic field, is capable of providing at least partial attitude control for gossamer spacecraft in polar orbit. In Sec. II the mathematical model from which the actuator torques are calculated was presented, and it was found that for a representative 100×100 m square structure, a conducting support structure carrying 10 A of current would be capable of enacting a maximum torque of 1.12 Nm. Simulation was then performed of a free, rigid structure in the presence of a magnetic field strength similar to that of the Earth's. This simulation demonstrated that the actuator torque magnitudes and directions were capable of detumbling the structure from an initial angular velocity of 0.1 rad s^{-1} within two days, and so could provide useful attitude control for large gossamer spacecraft.

The concept was developed with the application of orbital, solar reflectors in mind, and so further analysis was performed in Sec. III to assess whether it could provide attitude control for such reflectors. A simplified model was developed for a solar reflector in polar orbit, with magnetic field components given by a dipole model. It was found that the conducting structure could only partially provide the torques required to illuminate a target point continuously for the example spacecraft studied, but that if the areal mass density could be reduced by an order of magnitude then the system could provide full control of the reflector pitch angle. Further work could explore the minimum areal density required to provide structural support to a reflector and to carry the necessary current to provide magnetic control, which may prove to be the limiting factor. While the geometry of the reflector and target ground-point were constrained in this model, it did illustrate the operational concept and demonstrate the utility of the conducting structure. With further optimisation of the design, it could prove even more useful, particularly when the added benefits of distributed actuator torques and the potential ease of integration with the in-orbit fabrication process are taken into account.

V. Acknowledgements

B.R. acknowledges a PhD scholarship from the College of Science and Engineering, University of Glasgow, C.M. acknowledges support from a Royal Academy of Engineering Chair in Emerging Technologies and a Royal Society Wolfson Research Merit Award.

References

[1] Hoyt, R. P., "SpiderFab: an Architecture for Self-Fabricating Space Systems," *AIAA SPACE 2013 Conference and Exposition*, September 2013, pp. 1 – 17. doi:10.2514/6.2013-5509.

[2] Levedahl, B., Hoyt, R. P., Silagy, T., Gorges, J., Britton, N., and Slostad, J., "Trusselator™ Technology for In-Situ Fabrication of Solar Array Support Structures," *2018 AIAA Spacecraft Structures Conference*, January 2018. doi:10.2514/6.2018-2203.

[3] Billman, K. W., Gillbreath, W. P., and Bowen, S. W., "Introductory Assessment of Orbiting Reflectors for Terrestrial Power Generation," , NASA-TM-73230, 1977.

[4] McRobb, M., Robb, B., Ridley, S., and McInnes, C., "Emerging Space Technologies: Macro-scale On orbit Manufacturing," *17th Reinventing Space Conference - Belfast*, 12th - 14th November 2019.

[5] Fu, B., Gede, G., and Eke, F. O., "Controllability of a Square Solar Sail with Movable Membrane Tips," *Proceedings of the Institution of Mechanical engineers, Par G: Journal of Aerospace Engineering*, Vol. 231, No. 6, 2017, pp. 1065–1075. doi:10.1177/0954410016647533.

[6] Choi, M., and Damaren, C. J., "Structural Dynamics and Attitude Control of a Solar Sail Using Tip Vanes," *Journal of Spacecraft and Rockets*, Vol. 52, No. 6, 2015, pp. 1665–1679. doi:10.2514/1.A33179.

[7] Wie, B., "Solar Sail Attitude Control and Dynamics , Part 2," *Journal of Guidance Control and Dynamics*, Vol. 27, No. 4, 2004, pp. 536–544. doi:10.2514/1.11133.

[8] Borggräfe, A., Heiligers, J., Ceriotti, M., and McInnes, C. R., "Attitude control of large gossamer spacecraft using surface reflectivity modulation," *65th International Astronautical Congress*, Vol. 22, 2014, pp. 1753 – 1759. doi:10.1016/j.buildenv.2006.10.027.

[9] Gilbreath, W., Billman, K., and Bowen, S., "Enhanced Solar Energy Options using Earth-Orbiting Mirrors," *13th Intersociety Energy Conversion Engineering Conference*, August 1978, pp. 1528 – 1534.

[10] Lior, N., "Mirrors in the sky : Status , sustainability , and some supporting materials experiments," *Renewable and Sustainable Energy Reviews*, Vol. 18, 2013, pp. 401–415. doi:10.1016/j.rser.2012.09.008".

[11] Bonetti, F., and McInnes, C. R., "Space-Enhanced Solar Power for Equatorial Regions," *Advances in the Astronautical Sciences*, Vol. 160, 2017, pp. 3089 – 3107. doi:10.2514/1.A34032.

[12] Fraas, L. M., "Mirrors in space for low-cost terrestrial solar electric power at night," *2012 38th IEEE Photovoltaic Specialists Conference*, 2012, pp. 002862–002867. doi:10.1109/PVSC.2012.6318186.

[13] Fraas, L. M., "Sunbeams from mirrors in dawn-dusk orbit for earth solar power fields," *AIP Conference Proceedings*, Vol. 1556, No. 1, 2013, pp. 234–238. doi:10.1063/1.4822239.

[14] Robb, B., McRobb, M., and McInnes, C., "Distributed Magnetic Attitude Control for Large Gossamer Space Structures," *Submitted to Journal of Guidance, Control, and Dynamics*, 2019.

[15] Chulliat, A., Macmillan, S., Alken, P., Beggan, C., Nair, M., Hamilton, B., Woods, A., Ridley, V., Maus, S., and Thomson, A., "The US / UK World Magnetic Model for 2015-2020: Technical Report, National Geophysical Data Center, NOAA," , 2015. doi:10.7289/V5TB14V7.

[16] Wie, B., *Space Vehicle Dynamics and Control*, AIAA education series, American Institute of Aeronautics and Astronautics, 1998, pp. 425–444. doi:10.2514/4.860119.

[17] Stickler, A. S., "A Magnetic Control System for Attitude Acquisition," , NASA Report CR-130145, January 1972.

[18] Walt, M., *Introduction to Geomagnetically Trapped Radiation*, Cambridge Atmospheric and Space Science Series, Cambridge University Press, 2005, pp. 29 – 33.